



Prediction of Post-deformation Recrystallization Kinetics in AISI 321 Austenitic Stainless Steel Using Double-Stage Hot Compression

M. Shaban Ghazani and B. Eghbali

(Submitted August 13, 2018; in revised form May 12, 2019; published online June 18, 2019)

In the present research, a series of double-stage hot compression tests were conducted in the temperature range of 950–1150 °C, strain rates in the range of 0.01–1 s⁻¹, strain in the range of 0.1–0.3, and inter-pass time range of 3–100 s to evaluate the kinetics of the post-deformation recrystallization in AISI 321 austenitic stainless steel. An Avrami-type kinetics equation has been determined based on the obtained experimental data. Results show that the extent of post-deformation recrystallization increases with increase in inter-pass time, deformation temperature, pre-strain, and strain rate. The calculated activation energy for recrystallization (174 kJ/mol) is lower than the activation energy for static recrystallization of austenitic stainless steels. It is concluded that the both static and metadynamic recrystallization occurred during the inter-pass period. Also, the predicted softening fraction using the proposed kinetics equation agreed well with those obtained from experimental results.

Keywords AISI 321 steel, hot compression, kinetics equation, post-deformation recrystallization

1. Introduction

The grain size of metals and alloys, which is obtained by applying different types of thermomechanical processing including hot rolling, can be controlled by the occurrence of some well-known microstructural phenomena. The main microstructural evolution mechanisms occurring during hot deformation are dynamic recovery (DRV) (Ref 1), and dynamic recrystallization (DRX) (Ref 2). During the inter-pass period in hot rolling, microstructure is affected by other softening mechanisms which are generally called static softening processes (Ref 3). These mechanisms are static recovery (SRV) (Ref 4), static recrystallization (SRX) (Ref 5), and metadynamic recrystallization (MDRX) (Ref 6). During thermomechanical processing, different deformation parameters such as deformation temperature, strain, strain rate, and inter-pass time must be controlled precisely to achieve optimum combination of strength and toughness (Ref 7). In the case of austenite phase, the static recovery occurs at the early stages of the inter-pass period and only the 10–20 percent of static softening is related to occurrence of static recovery. But the occurrence of static and metadynamic recrystallization depends on the extent of the applied strain in the previous deformation pass (Ref 8). If the imposed strain is lower than the critical strain for initiation of dynamic recrystallization (ϵ_c), the static recovery is accom-

panied by the occurrence of static recrystallization (Ref 9), whereas the metadynamic recrystallization occurs when the applied strain is higher than the critical strain (ϵ_c) (Ref 10). Metadynamic recrystallization occurs as a result of the continued growth of the nuclei of dynamic recrystallization formed during the previous deformation stage (Ref 11). When metadynamic recrystallization is the prevailing static softening phenomenon ($\epsilon > \epsilon_c$), the static recovery and static recrystallization occur concurrently in the deformed austenite matrix. Therefore, the combination of static and metadynamic recrystallization is named as post-deformation recrystallization (Ref 12). By inspection of the available literature, it is revealed that the numerous studies were focused on the dynamic recrystallization behavior of austenitic stainless steels. For example, Dehghan-Manshadi et al. (Ref 13) showed that while dynamic recrystallization of AISI 304 austenitic stainless steel starts at a strain as low as 60 percent of the peak strain, a fully recrystallized microstructure needs a high strain of almost 4.5 times the initiation strain. Nkhoma et al. (Ref 14) compared the hot workability of AISI 304 and AISI 321 steel through the execution of single pass hot deformation in the temperature range of 800–1200 °C. They showed that the AISI 321 steel is slightly softer than the AISI 304 steel and their deformation activation energies were calculated to be 465 and 446 kJ/mol, respectively. Guo et al. (Ref 15) studied the hot deformation behavior of AISI 316LN steel in the temperature range of 900–1200 °C and strain rates in the range of 0.001–10 s⁻¹. Their results showed that the peak stress decreases with increase in the deformation temperature and decrease in strain rate and the initial austenitic grain size has little influence on the peak stress. Furthermore, there is little information on the post-deformation softening behavior of austenitic stainless steels. Dehghan-Manshadi et al. (Ref 16) studied the metadynamic recrystallization behavior of AISI 304 steel through the double-stage hot torsion testing. Their results indicated that the time for 50% recrystallization changes from strain dependent to strain independent at a transition strain. Miao et al. (Ref 17) investigated the static recrystallization behavior of 316LN steel

M. Shaban Ghazani, Department of Materials Science Engineering, University of Bonab, P.O. Box 5551761167, Bonab, Iran; and B. Eghbali, Faculty of Materials Science and Engineering, Sahand University of Technology, P.O. Box 51335-1996, Tabriz, Iran. Contact e-mail: eghbali@sut.ac.ir.

and showed that deformation temperature has significant influence on static recrystallization and the volume fraction of recrystallization could easily reach 100% at higher deformation temperatures. Their results indicated that the activation energy for static recrystallization is about 317 kJ/mol. Although the dynamic recovery (Ref 18) and dynamic recrystallization (Ref 19, 20) behaviors of AISI 321 austenitic stainless steel have been studied by current authors, there is not any information regarding the post-deformation recrystallization behavior of this grade of austenitic stainless steels. Therefore, in the present work, the kinetics of the post-deformation recrystallization of AISI 321 steel was evaluated using the double-stage hot compression deformation. The results of this study can be used in the optimization of the process parameters during multi-step hot rolling to control the extent of the static softening during the holding period of different rolling stages.

2. Material and Experimental Procedure

Chemical composition of the AISI 321 austenitic stainless steel used in the present investigation is shown in Table 1. As can be seen, the 0.32 wt.% titanium was added to this grade of stainless steel to reduce the grain boundary sensitization which is the common corrosion phenomenon in other un-stabilized grades such as AISI 304 and 316 steels (Ref 21, 22). Cylindrical samples with 15 mm height and 10 mm diameter were machined from as received rod. As the raw material was received in the form of the cold deformed rod, the initial microstructure consisted of cold deformed austenite phase with deformation twins and also strain-induced martensite (Fig. 1a). In order to achieve uniform microstructure with equiaxed austenite grains and elimination of the deformation-induced martensite just before double-stage deformation, samples were annealed at 1200 °C for 10 min. The short heating time of 10 min was selected to prevent intensive austenite grain growth. Figure 1(b) shows the annealed microstructure of samples just before thermomechanical processing. It is seen that the annealed microstructure consisted of equiaxed austenite grains in conjunction with annealing twins and TiN inclusions. The double-stage hot compression tests were then performed on cylindrical samples using Zwick–Roell Z250 testing machine. The schematic representation of the thermomechanical procedure used in the present study is illustrated in Fig. 2. As shown in Fig. 2, samples were heated at the rate of 10 °C/s to the specified deformation temperature and held for 5 min to achieve uniform temperature distribution inside sample. Then, the first step of compression test was performed at the constant strain rate up to the predefined strain. After the holding time, the second stage of deformation was conducted at the same temperature and strain rate of the first stage up to the accumulated strain of 0.7. Samples were quenched in water after the second deformation stage. To evaluate the effects of deformation temperature, pre-strain and strain rate on the extent

of post-deformation softening, hot compression tests were performed in the temperature range of 950–1150 °C, pre-strain in the range of 0.1–0.3, and strain rates in the range of 0.01–1 s⁻¹. Force–displacement curves obtained from double-stage hot deformations were converted to true stress–true strain curves, and the extent of post-deformation softening was evaluated using the 0.2% offset stress method (Ref 23).

3. Results and Discussion

3.1 Double-Stage Hot Compression Curves

The variations of the flow stress of AISI 321 austenitic steel during the first and second stages of hot compression deformation are shown in Fig. 3. Also, the effects of deformation parameters on double-stage hot compression curves are depicted. The effect of inter-pass time can be elucidated from Fig. 3(a). As it is evident, the level of flow stresses during first stage of deformation is the same in all tests due to the identical deformation parameters. However, it is seen that the flow stress in the second stage is decreased with increase in inter-pass time. This is attributed to the thermally activated microstructural evolutions occurring during the delay time between these two passes. The main softening mechanisms leading to the lower flow stress in the second stage of deformation are static recovery, static and metadynamic recrystallization (Ref 8). Figure 3(b) indicates that the flow stress in both first and second stages increases with decrease in deformation temperature. Therefore, it can be deduced that the microstructural evolutions during hot deformation are also based on thermally activated mechanisms. It is well understood that the flow behaviors of materials during hot deformation are controlled mainly by work hardening and the occurrence of dynamic recovery and recrystallization (Ref 24). Therefore, increasing deformation temperature provides more activation energy for dynamic recovery and recrystallization and these results in lower flow stress levels. It is also apparent in Fig. 3(a) that the flow curve in the second stage of deformation at the temperature of 1150 °C shows a peak stress which is the main indication of the occurrence of dynamic recrystallization. The effects of strain rate on flow curves at a constant deformation temperature of 1050 °C are shown in Fig. 3(c). It can be observed that the flow stress level in both first and second stage of hot compression increases with increase in strain rate.

3.2 Calculation of Softening Fraction

The amount of softening due to the occurrence of static recovery, metadynamic and static recrystallization can be calculated using the flow stress levels of first and second stages of hot compression deformation. Four different methods were proposed to relate the difference of the flow stress in the first and second stage to the amount of static softening. These methods include offset stress method, strain recovery method,

Table 1 The chemical composition of the AISI 321 steel used in the present work (wt.%)

C	Cr	Ni	Mo	Ti	Mn	Si	S	P	N	Fe
0.04	18.16	10.52	0.24	0.32	1.87	0.36	0.018	0.026	0.001	Bal.

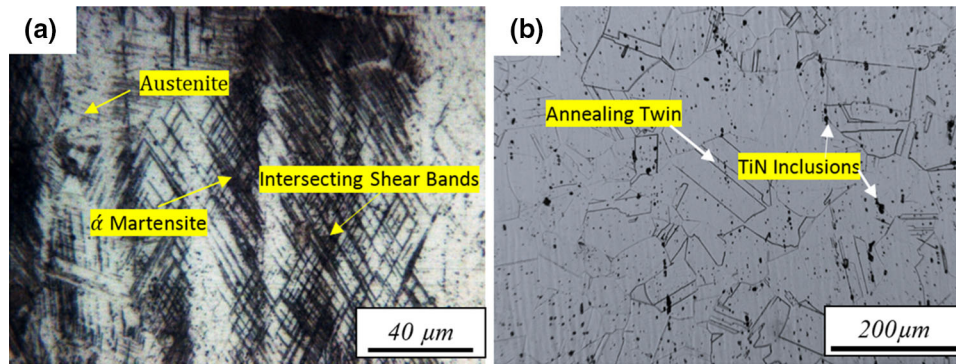


Fig. 1 Microstructures of AISI 321 austenitic stainless steel: (a) as received and (b) after annealing for 10 min at 1200 °C

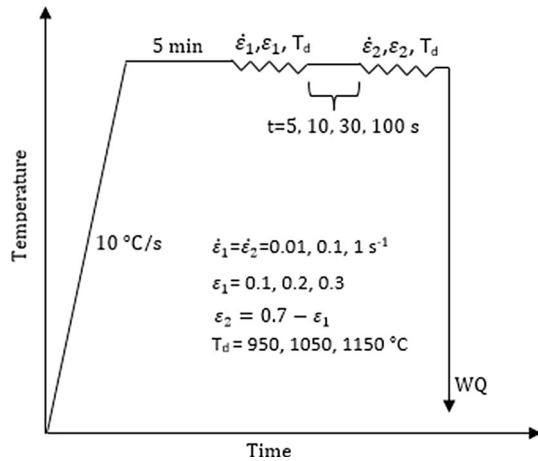


Fig. 2 Schematic of the thermomechanical procedure used in the present research

back extrapolation method, and average stress method (Ref 25). In the present investigation, the 0.2% offset yield stress method was used for determination of the amount of softening. The schematic representation of the offset yield stress method is shown in Fig. 4. According to this method, the amount of static softening is determined using the following equation (Ref 26):

$$SF = \frac{\sigma_m - \sigma_2}{\sigma_m - \sigma_1} \quad (\text{Eq 1})$$

where σ_m is the flow stress level at the end of the first step, σ_1 and σ_2 are the 0.2% offset stress of the first and second stages, respectively (Fig. 4). The variations of static softening percentage with inter-pass delay times under different deformation conditions (strain rate, temperature, and strain) are shown in Fig. 5. It is obvious that the softening percentage increases with increase in deformation temperature and inter-pass delay time (Fig. 5(a)) because the static softening mechanisms, including recovery and recrystallization, are thermal activated. The maximum softening percentages after 100 s inter-pass delay at temperatures of 950, 1050, and 1150 °C are 32.6, 62.5, and 89.4%, respectively. Therefore, it can be concluded that the post-deformation recrystallization is partial after 100 s delay at all the investigated temperatures. It is also seen that the softening percentage increases slowly at the early stage of inter-pass period and the softening rate increases rapidly with the further increase in the delay time. Figure 5(b) shows the

variations of softening percentage with inter-pass delay time at different strain rates. It is clear that the amount of static softening increases with increase in strain rate. Therefore, the higher amount of softening occurs at the strain rate of 1 s^{-1} compared with other strain rates. This is due to the fact that the extent of dynamic recovery during first stage of deformation is reduced with increase in strain rate as a result of the lower time available for cross slip and climb of dislocations. So, the higher dislocation density obtained just after the first step of double-stage compression test increases the driving force for post-deformation recovery and recrystallization during the inter-pass period. Figure 5(c) illustrates the effect of pre-strain on the softening percentage. For this purpose, the strains of the first deformation stage were selected to be 0.1, 0.2, and 0.3 and the double-stage deformations were performed at the temperature of 1050 °C and strain rate of 0.1 s^{-1} . It is clear that the amount of static softening including recovery and recrystallization is increased with pre-strain. This is mainly due to the generation of more dislocation densities at higher strains, which provides a driving force for static softening mechanisms. For further confirmation of the results of static softening percentage obtained by double-stage compression, the microstructures of AISI 321 austenitic stainless steel after deformation with different pre-strains are represented in Fig. 6. Optical microstructure of AISI 321 steel after 100 s inter-pass period with the pre-strain of 0.1 is shown in Fig. 6(a). As can be seen, the entire microstructure consisted of slightly deformed austenite grains. The fine austenite grains resulting from recrystallization are not observed in this micrograph. From Fig. 5(c), the softening percentage at this condition is about 17% which is in accordance with the observed microstructure. It has been mentioned in the literature that the 10-20% of inter-pass softening during double-stage deformation can be attributed to the occurrence of static recovery (Ref 27). Figure 6(b) shows the microstructure of AISI 321 steel after 100 s inter-pass period which was deformed with the pre-strain of 0.2. In this micrograph, both deformed and fine equiaxed austenite grains are observable. The calculated softening percentage at this condition is about 62% (Fig. 5c) and seems reasonable when compared with the obtained microstructure. Microstructure obtained after 100 s inter-pass period and pre-strain of 0.3 consisted mainly of fine equiaxed and some elongated austenite grains (Fig. 6c). The softening percentage is about 93% considering the results represented in Fig. 5(c). These equiaxed austenite grains are expected to be formed as a result of the occurrence of metadynamic recrystallization because the

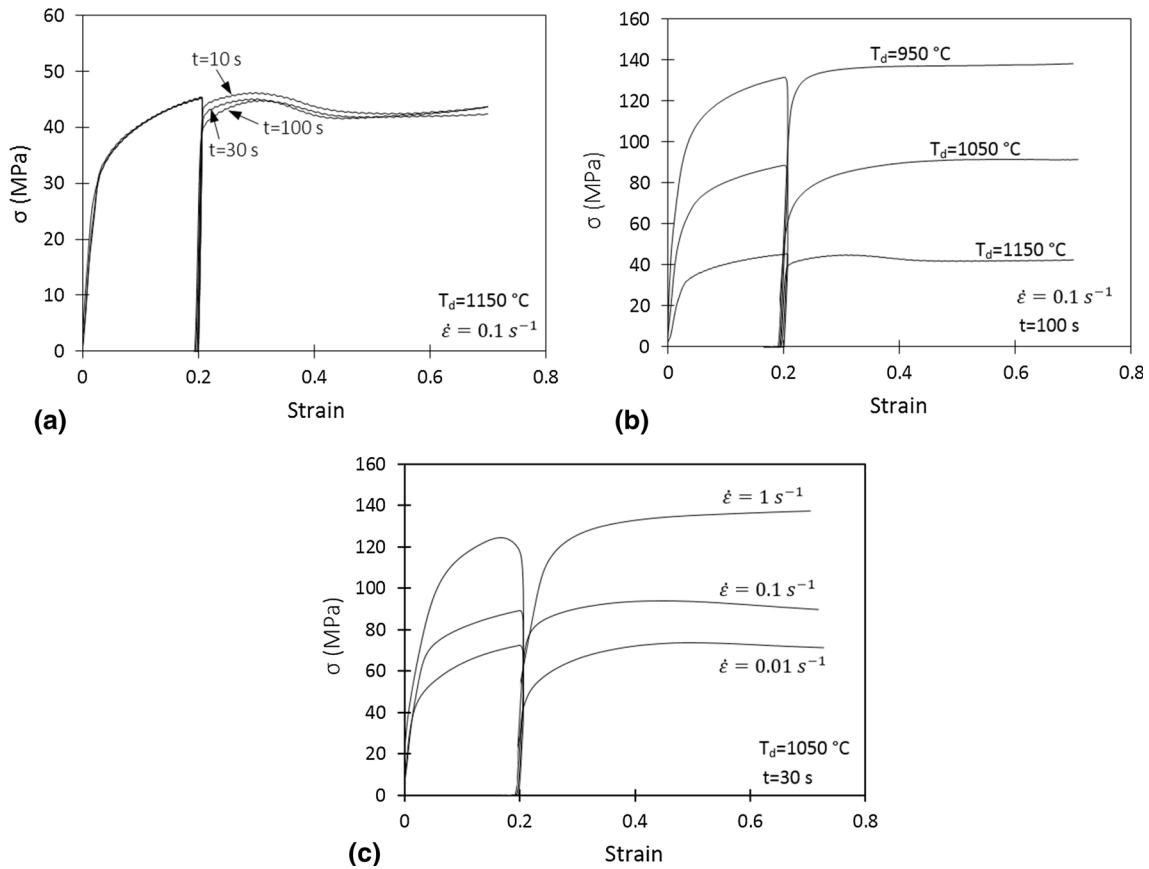


Fig. 3 The effect of different deformation parameters on double-stage hot compression curves: (a) inter-pass time, (b) deformation temperature, and (c) strain rate

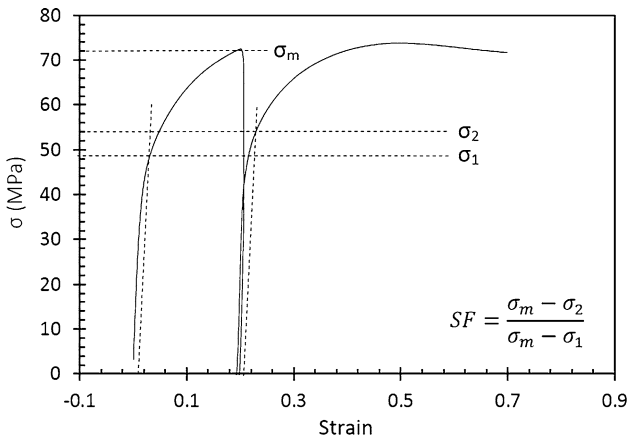


Fig. 4 Determination of softening fraction using 0.2% yield stress

applied pre-strain is higher than the critical strain for the occurrence of dynamic recrystallization during first deformation stage (Ref 20).

3.3 Kinetics of Post-deformation Recrystallization

For determination of the kinetics of post-deformation recrystallization, it was assumed that the 10% of the softening during an inter-pass period is due to the static recovery. Therefore, the post-deformation recrystallization fraction (X_{PDRX}) can be obtained using the following equation (Ref 27):

$$X_{\text{PDRX}} = \frac{\text{SF} - 0.1}{0.9} \quad (\text{Eq 2})$$

where the SF is the softening fraction calculated directly from double-stage hot compression tests (Fig. 4). The kinetics of post-deformation recrystallization can be expressed using the Avrami-type equation in the following form (Ref 16):

$$X_{\text{PDRX}} = 1 - \exp \left[-0.693 \left(\frac{t}{t_{0.5}} \right)^n \right] \quad (\text{Eq 3})$$

where t is time, n is Avrami exponent, and $t_{0.5}$ is the time required for 50% static recrystallization. The following expression is obtained by taking logarithm on both sides of Eq 3:

$$\ln \left(\ln \left(\frac{1}{1 - X_{\text{PDRX}}} \right) \right) = \ln(-0.693) + n \ln(t) - n \ln(t_{0.5}) \quad (\text{Eq 4})$$

According to Eq 4, the value of the Avrami exponent (n) can be calculated from the slope of the $\ln \left(\ln \left(\frac{1}{1 - X_{\text{PDRX}}} \right) \right)$ versus $\ln(t)$ curves. Figure 7 represents these curves which were obtained by substituting the X_{PDRX} and t values in Eq 4. The Avrami exponent was then determined from the average slope of these curves ($n = 0.775$).

The applied pre-strain in the present investigation is in the range of 0.1-0.3. It should be noted that the strain of 0.1 is lower than critical strain for initiation of dynamic recrystallization. Therefore, static recrystallization occurs during the

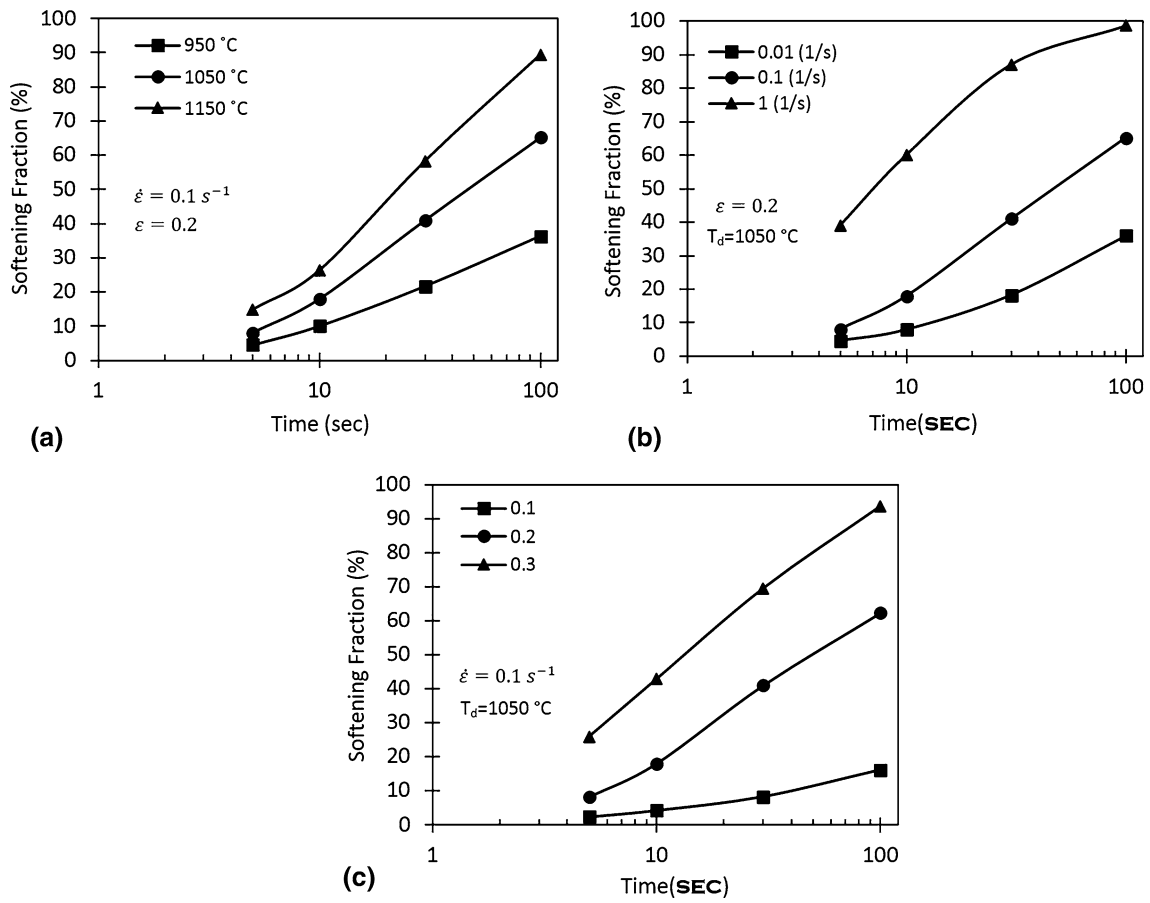


Fig. 5 The effect of deformation parameters on the amount of static softening percentage during inter-pass time: (a) deformation temperature, (b) strain rate, and (c) strain

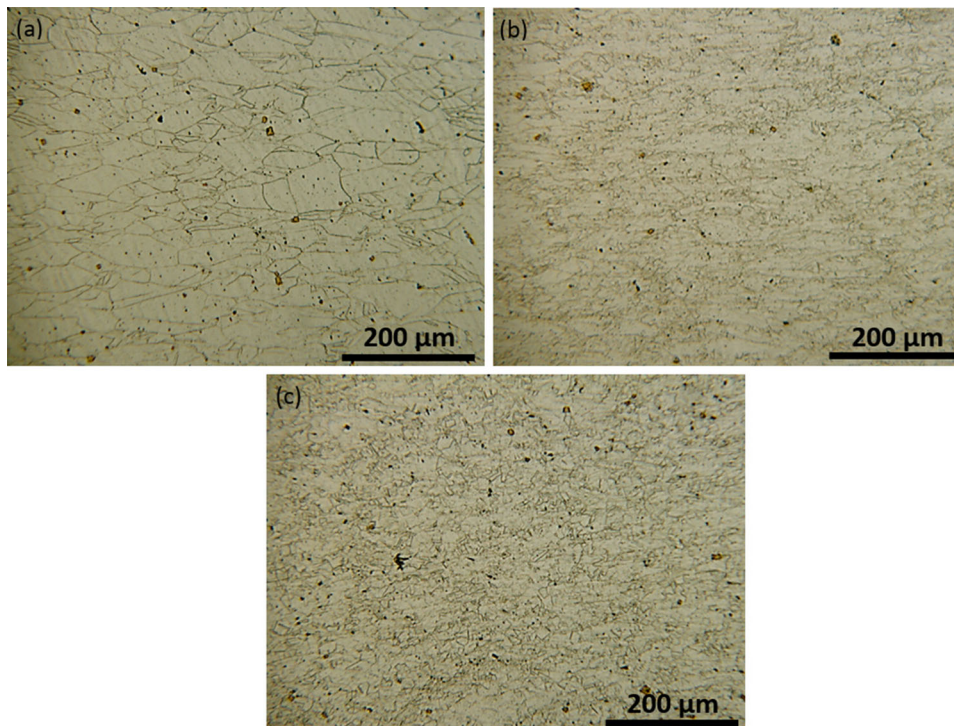


Fig. 6 Effect of pre-strain on the microstructure of AISI 321 austenitic stainless steel subjected to double-stage compression deformation with strain rate of 0.1 s⁻¹, deformation temperature of 1050 °C and inter-pass time of 100 s: (a) $\epsilon = 0.1$, (b) $\epsilon = 0.2$ and (c) $\epsilon = 0.3$

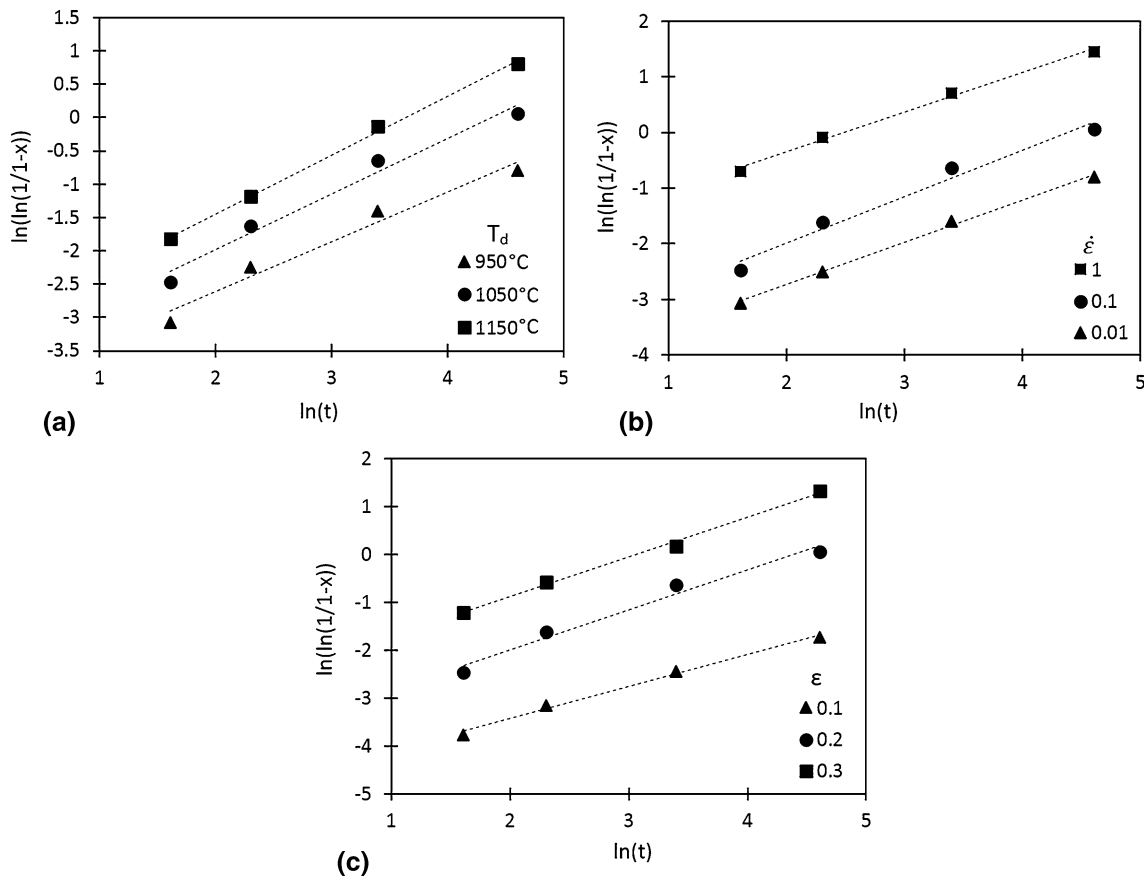


Fig. 7 The $\ln(\ln(1/(1-x)))$ vs. $\ln(t)$ curves obtained from double-stage hot compression at different deformation parameters: (a) temperature, (b) strain rate, and (c) strain

holding period, whereas the applied strain of 0.3 is higher than the critical strain so that the metadynamic recrystallization occurs under these conditions. It is concluded that the post-deformation softening is due to the occurrence of the both of static and metadynamic recrystallization. Therefore, the time for 50% post-deformation softening was found to vary with strain and strain rate. So, the following expression was used to express the time required for 50% softening (Ref 17):

$$t_{0.5} = A\dot{\epsilon}^p \epsilon^q \exp\left(\frac{Q_{\text{PDRX}}}{RT}\right) \quad (\text{Eq 5})$$

where A , p , and q are material constants, Q_{PDRX} is the activation energy of post-deformation softening, R is universal gas constant, T is absolute deformation temperature, $\dot{\epsilon}$ is strain rate, and ϵ is applied strain. Following expression is obtained by taking logarithm on both sides of the above equation:

$$\ln(t_{0.5}) = \ln A + p \ln(\dot{\epsilon}) + q \ln(\epsilon) + \frac{Q_{\text{PDRX}}}{RT} \quad (\text{Eq 6})$$

The values of $t_{0.5}$ were obtained under different deformation conditions from the intercept of the $\ln\left(\ln\left(\frac{1}{1-X_{\text{PDRX}}}\right)\right)$ versus $\ln(t)$ curves. After determination of the value of the time required for 50% recrystallization ($t_{0.5}$), the $\ln(t_{0.5})$ versus $\ln \dot{\epsilon}$, $\ln(t_{0.5})$ versus $\ln(\epsilon)$ and $\ln(t_{0.5})$ versus $\frac{1}{T}$ curves were plotted and the values of p , q , and Q_{PDRX} were obtained from the slope of these curves, respectively (Fig. 8). Also, the value of $\ln A$ in Eq 6 was determined from the intercept of the $\ln(t_{0.5})$ versus $\frac{1}{T}$ curves.

Finally, the kinetics equations for post-deformation recrystallization of AISI 321 austenitic stainless steel in the temperature range of 950-1150 °C were determined as given below:

$$X_{\text{PDRX}} = 1 - \exp\left[-0.693\left(\frac{t}{t_{0.5}}\right)^{0.775}\right]$$

$$t_{0.5} = 3.24 \times 10^{-9} \dot{\epsilon}^{-0.6819} \epsilon^{-3.8256} \exp\left(\frac{174000}{RT}\right) \quad (\text{Eq 7})$$

The activation energy for post-deformation recrystallization of AISI 321 austenitic stainless steel in the present investigation is calculated to be 174 kJ/mol which is lower than the activation energy for static recrystallization of austenitic stainless steels. For example, Miao et al. (Ref 17) studied the hot deformation behavior of 316LN steel and their investigation showed that the activation energy of static recrystallization is about 317 kJ/mol. Also, in another study conducted by Cho et al. (Ref 28) the activation energy of metadynamic recrystallization in austenitic stainless steel was determined to be about 230 kJ/mol. It is seen that the activation energy of post-deformation recrystallization in AISI 321 steel is near the activation energy of metadynamic recrystallization of austenitic stainless steels. Therefore, it is concluded that most of the softening occurs due to the metadynamic recrystallization. But, it must be noted that the pre-strains in the first deformation step ($\epsilon = 0.1, 0.2$, and 0.3) are in the range for the occurrence of both static and metadynamic recrystallization. In another work

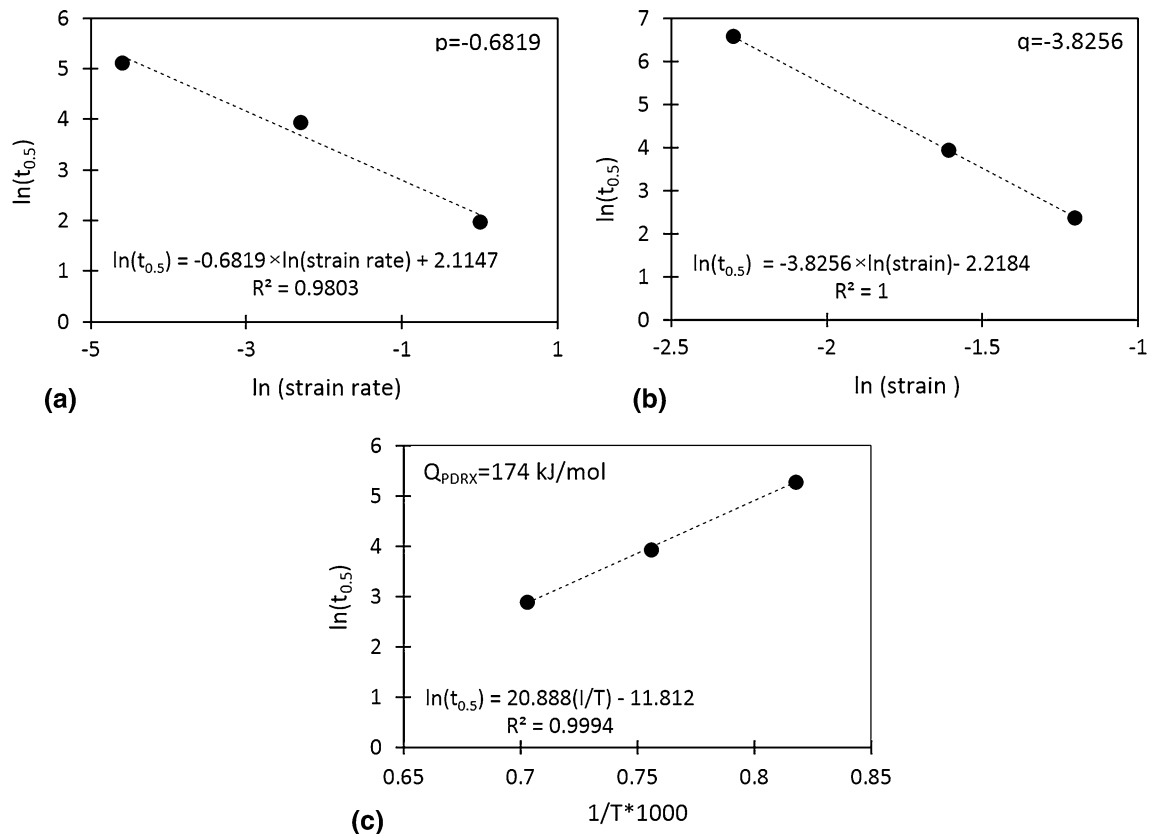


Fig. 8 The plots of: (a) $\ln(t_{0.5})$ vs. $\ln \dot{\epsilon}$, (b) $\ln(t_{0.5})$ vs. $\ln(\epsilon)$ and (c) $\ln(t_{0.5})$ vs. $\frac{1}{T}$ for determination of the material-dependent constants in Eq 6

conducted by authors (Ref 20), the critical strains for the onset of dynamic recrystallization in AISI 321 steel were calculated at different deformation conditions. Comparing the pre-strain values in the first step of hot deformation with critical strains determined at the specified conditions shows that the strain of 0.1 is lower than the critical strain for the onset of dynamic recrystallization. So, it is deduced that the static recrystallization is the prevailing softening mechanism, whereas the pre-strain of 0.3 is higher than the critical strain for the onset of dynamic recrystallization. Therefore, the metadynamic recrystallization is expected to occur during the inter-pass period. The lower activation energy obtained in the present study can be attributed to the subtraction of the effect of static recovery from the values of softening fraction. Also, the lower activation energy results from the differences in the chemical composition of AISI 321 steel with other grades of austenitic stainless steels. The investigated steel has about 0.32 wt.% titanium, which is a strong carbonitride forming element. It has been demonstrated that dynamic recovery and dynamic recrystallization of austenite phase are retarded by titanium addition (Ref 29). This results in the higher dislocation density in the microstructure of austenite just after the first step and before inter-pass initiation. Higher dislocation density provides more driving force for static restoration processes and reduces the amount of activation energy required for the occurrence of recrystallization during the inter-pass period.

3.4 Comparing the Predicted and Experimental Results

Figure 9 represents the variations of the predicted values of the post-deformation softening percentage with inter-pass time

at a constant temperature, strain rate, and strain. As can be seen, the variations of the softening percentage show a trend similar to the Avrami-type behavior. Also, the experimental amounts of the softening percentage are shown as dotted values for comparison propose. It is seen that the predicted values are in good agreement with the experimental result. Therefore, the proposed kinetic equation can be used for estimation of the post-deformation softening fraction during the hot deformation of AISI 321 austenitic stainless steel.

4. Conclusions

In the present investigation, the effect of hot deformation parameters, namely the pre-strain, strain rate, and temperature on the kinetics of post-deformation softening in AISI 321 austenitic stainless steel, was investigated using the double-stage hot compression test in the temperature range of 950–1150 °C. The main results are as given below:

1. The flow stress of AISI 321 steel during first and second stages of hot deformation is affected by processing parameters. The flow stress increases with decrease in deformation temperature and increase in strain rate and decrease in inter-pass time.
2. The experimental results show that the extent of inter-pass softening increased with increase in deformation temperature, strain rate, and pre-strain. This indicates that softening occurred through the thermal activated microstructural evolution.

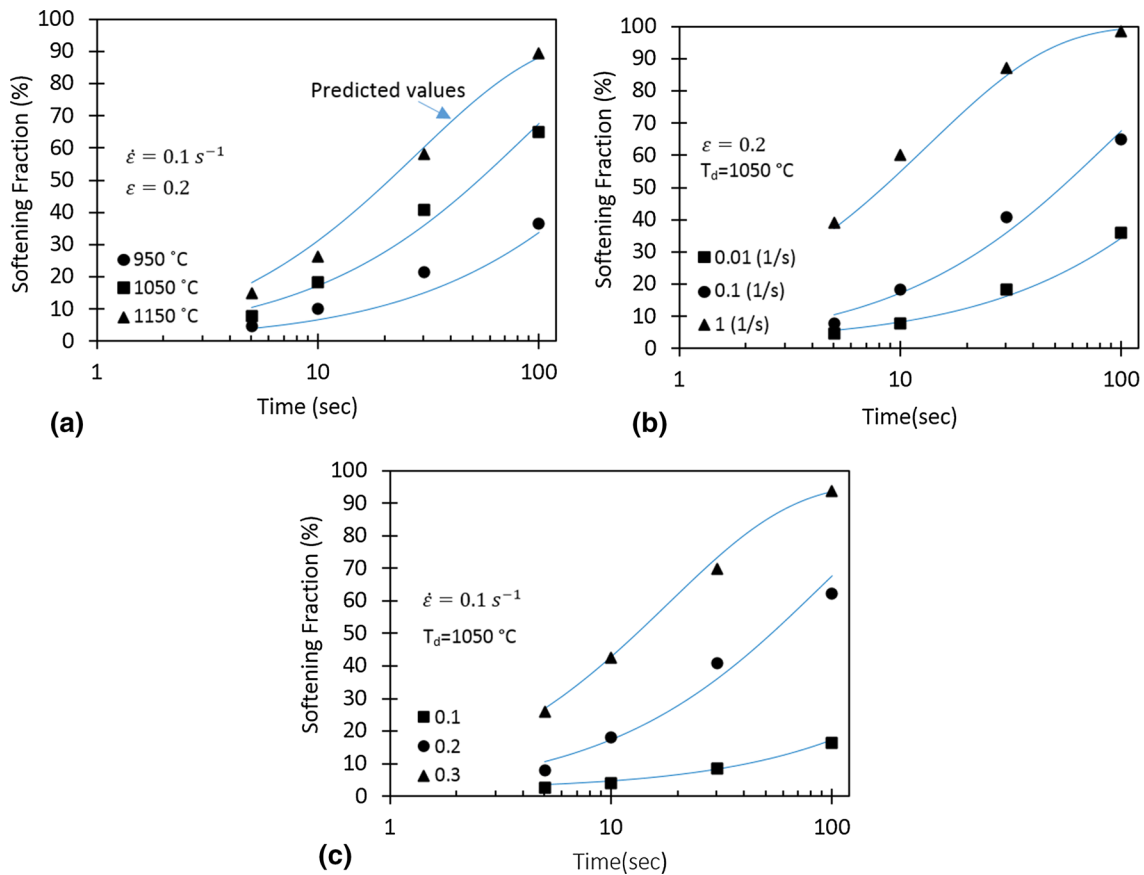


Fig. 9 Comparing the predicted static softening percentage using the obtained kinetic equation and experimental values: (a) effect of deformation temperature, (b) effect of strain rate, and (c) effect of pre-strain

- The kinetics of post-deformation recrystallization was evaluated using the Avrami-type equation. The following expressions were obtained to express the variations of the recrystallization fraction during the inter-pass period:

$$X_{\text{PDRX}} = 1 - \exp \left[-0.693 \left(\frac{t}{t_{0.5}} \right)^{0.775} \right]$$

$$t_{0.5} = 3.24 \times 10^{-9} \dot{\epsilon}^{-0.6819} \epsilon^{-3.8256} \exp \left(\frac{174000}{RT} \right)$$

- The activation energy for post-deformation recrystallization of AISI 321 steel was calculated to be 174 kJ/mol and is lower than the activation energy for static recrystallization of other grades of austenitic stainless steels and also near the activation energy of metadynamic recrystallization. This shows that the metadynamic recrystallization is the predominant softening phenomenon for the deformation conditions used in the present study.
- The time required for 50% softening of AISI 321 steel during the inter-pass period is dependent on strain rate and pre-strain. This indicates that both static and metadynamic recrystallization occurred during the inter-pass period.
- Comparing the predicted and experimental results, it is concluded that the proposed kinetic equation predicts the

post-deformation softening fraction of the AISI 321 steel accurately.

References

- H. McQueen and W. Blum, Dynamic Recovery: Sufficient Mechanism in the Hot Deformation of Al (< 99.99), *Mater. Sci. Eng. A*, 2000, **290**, p 95–107
- T. Al-Samman and G. Gottstein, Dynamic Recrystallization during High Temperature Deformation of Magnesium, *Mater. Sci. Eng. A*, 2008, **490**, p 411–420
- H. Zhang, G. Lin, D. Peng, L. Yang, and Q. Lin, Dynamic and Static Softening Behaviors of Aluminum Alloys during Multistage Hot Deformation, *J. Mater. Process. Technol.*, 2004, **148**, p 245–249
- T. Sakai, M. Ohashi, K. Chiba, and J. Jonas, Recovery and Recrystallization of Polycrystalline Nickel After Hot Working, *Acta Metall.*, 1988, **36**, p 1781–1790
- Y. Lin, M.-S. Chen, and J. Zhong, Study of Static Recrystallization Kinetics in a Low Alloy Steel, *Comput. Mater. Sci.*, 2008, **44**, p 316–321
- S. Medeiros, Y. Prasad, W.G. Frazier, and R. Srinivasan, Microstructural Modeling of Metadynamic Recrystallization in Hot Working of IN 718 Superalloy, *Mater. Sci. Eng. A*, 2000, **293**, p 198–207
- M. Jahazi and B. Egbali, The Influence of Hot Rolling Parameters on the Microstructure and Mechanical Properties of an Ultra-high Strength Steel, *J. Mater. Process. Technol.*, 2000, **103**, p 276–279
- S.H. Cho, K.-B. Kang, and J.J. Jonas, The Dynamic, Static and Metadynamic Recrystallization of a Nb-Microalloyed Steel, *ISIJ Int.*, 2001, **41**, p 63–69

9. H. Mao, R. Zhang, L. Hua, and F. Yin, Study of Static Recrystallization Behaviors of GCr15 Steel Under Two-Pass Hot Compression Deformation, *J. Mater. Eng. Perform.*, 2015, **24**, p 930–935
10. C. Zhang, L. Zhang, W. Shen, C. Liu, and Y. Xia, The Kinetics of Metadynamic Recrystallization in a Ni-Cr-Mo-Based Superalloy Hastelloy C-276, *J. Mater. Eng. Perform.*, 2016, **25**, p 545–552
11. H. McQueen, Development of Dynamic Recrystallization Theory, *Mater. Sci. Eng. A*, 2004, **387**, p 203–208
12. A. Taylor and P. Hodgson, The Post-deformation Recrystallization Behaviour of 304 Stainless Steel Following High Strain Rate Deformation, *Mater. Sci. Eng. A*, 2011, **529**, p 164–169
13. A. Dehghan-Manshadi, M.R. Barnett, and P. Hodgson, Hot Deformation and Recrystallization of Austenitic Stainless Steel: Part I. Dynamic Recrystallization, *Metall. Mater. Trans. A*, 2008, **39**, p 1359–1370
14. R.K. Nkhoma, C.W. Siyasiya, and W.E. Stumpf, Hot Workability of AISI, 321 and AISI, 304 Austenitic Stainless Steels, *J. Alloys Compd.*, 2014, **595**, p 103–112
15. B. Guo, H. Ji, X. Liu, L. Gao, R. Dong, M. Jin, and Q. Zhang, Research on Flow Stress during Hot Deformation Process and Processing Map for 316LN Austenitic Stainless Steel, *J. Mater. Eng. Perform.*, 2012, **21**, p 1455–1461
16. A. Dehghan-Manshadi, M.R. Barnett, and P. Hodgson, Hot Deformation and Recrystallization of Austenitic Stainless Steel: Part II. Post-deformation Recrystallization, *Metall. Mater. Trans. A*, 2008, **39**, p 1371–1381
17. J. Miao, L. Bo, X.-g. LIU, G. Huan, H.-p. JI, B.-f. GUO, Static recrystallization behavior of 316LN austenitic stainless steel, *Journal of Iron and Steel Research, International* 20 (2013) 67-72
18. M.S. Ghazani, B. Eghbali, and G.R. Ebrahimi, Evaluation of the Kinetics of Dynamic Recovery in AISI, 321 Austenitic Stainless Steel Using Hot Flow Curves, *Trans. Indian Inst. Met.*, 2017, **70**, p 1755–1761
19. M.S. Ghazani and B. Eghbali, Characterization of the Hot Deformation Microstructure of AISI, 321 Austenitic Stainless Steel, *Mater. Sci. Eng. A*, 2018, **730**, p 380–390
20. M.S. Ghazani, B. Eghbali, and G. Ebrahimi, Kinetics and Critical Conditions for Initiation of Dynamic Recrystallization during Hot Compression Deformation of AISI, 321 Austenitic Stainless Steel, *Met. Mater. Int.*, 2017, **23**, p 964–973
21. R. Singh, I. Chatteraj, A. Kumar, B. Ravikumar, and P.K. Dey, The Effects of Cold Working on Sensitization and Intergranular Corrosion Behavior of AISI, 304 Stainless Steel, *Metall. Mater. Trans. A*, 2003, **34**, p 2441–2447
22. J. Stella, J. Cerezo, and E. Rodríguez, Characterization of the Sensitization Degree in the AISI, 304 Stainless Steel Using Spectral Analysis and Conventional Ultrasonic Techniques, *NDT and E Int.*, 2009, **42**, p 267–274
23. A. Yanagida, J. Yanagimoto, Formularization of softening fractions and related kinetics for static, *Materials Science and Engineering A* 487 (2008) 510-517. recrystallization using inverse analysis of double compression test
24. T. Furuhashi, B. Poorganji, H. Abe, and T. Maki, Dynamic Recovery and Recrystallization in Titanium Alloys by Hot Deformation, *JOM*, 2007, **59**, p 64–67
25. K. Rao, Y. Prasad, and E.B. Hawbolt, Study of Fractional Softening in Multi-stage Hot Deformation, *J. Mater. Process. Technol.*, 1998, **77**, p 166–174
26. Y.C. Lin, L.-T. Li, and Y.-C. Xia, A New Method to Predict the Metadynamic Recrystallization Behavior in 2124 Aluminum Alloy, *Comput. Mater. Sci.*, 2011, **50**, p 2038–2043
27. H.J. McQueen and J.J. Jonas, Role of the Dynamic and Static Softening Mechanisms in Multistage Hot Working, *J. Appl. Metalwork.*, 1985, **3**, p 410–420
28. S.-H. Cho and Y.-C. Yoo, Metadynamic Recrystallization of Austenitic Stainless Steel, *J. Mater. Sci.*, 2001, **36**, p 4279–4284
29. M. Arribas, B. López, and J. Rodríguez-Ibabe, Additional Grain Refinement in Recrystallization Controlled Rolling of Ti-Microalloyed Steels Processed by Near-Net-Shape Casting Technology, *Mater. Sci. Eng. A*, 2008, **485**, p 383–394

Publisher's Note Springer Nature remains neutral with regard to jurisdictional claims in published maps and institutional affiliations.